Check for updates

ADVANCING EARTH AND SPACE SCIENCE

Geophysical Research Letters

RESEARCH LETTER

10.1029/2021GL094739

Key Points:

- Community Earth Systems Model versions 1.1 and 2 significantly underestimate decadal surface freshening in the Canada Basin
- The surface freshening model bias is likely not related to seasonal freshwater input at the surface from sea ice melt or other sources
- The models distribute freshwater over an unrealistically large depth range in recent years, which contributes to the surface salinity bias

Supporting Information:

Supporting Information may be found in the online version of this article.

Correspondence to:

E. Rosenblum,
erica.j.rosenblum@gmail.com

Citation:

Rosenblum, E., Fajber, R., Stroeve, J. C., Gille, S. T., Tremblay, L. B., & Carmack, E. C. (2021). Surface salinity under transitioning ice cover in the Canada Basin: Climate model biases linked to vertical distribution of fresh water. *Geophysical Research Letters*, *48*, e2021GL094739. https://doi.org/10.1029/2021GL094739

Received 7 JUN 2021
Accepted 8 OCT 2021

© 2021. The Authors.
This is an open access article under the terms of the Creative Commons Attribution-NonCommercial-NoDerivs License, which permits use and distribution in any medium, provided the original work is properly cited, the use is non-commercial and no modifications or adaptations are made.

Surface Salinity Under Transitioning Ice Cover in the Canada Basin: Climate Model Biases Linked to Vertical Distribution of Fresh Water

E. Rosenblum[1], R. Fajber[2], J. C. Stroeve[1,3,4], S. T. Gille[5], L. B. Tremblay[6], and E. C. Carmack[7]

[1]Centre for Earth Observation Science, University of Manitoba, Winnipeg, MB, Canada, [2]University of Washington, Seattle, WA, USA, [3]Centre for Polar Observation and Modelling, University College London, Earth Sciences, London, UK, [4]National Snow and Ice Data Center, Cooperative Institute for Research in Environmental Sciences, University of Colorado, Boulder, CO, USA, [5]Scripps Institution of Oceanography, University of California San Diego, La Jolla, CA, USA, [6]Department of Atmospheric Science, McGill University, Montreal, QC, Canada, [7]Fisheries and Oceans Canada, Sidney, BC, Canada

Abstract The Canada Basin has exhibited a significant trend toward a fresher surface layer and thus a more stratified upper-ocean over the past three decades. State-of-the-art ice-ocean models, by contrast, tend to simulate a surface layer that is saltier and less stratified than observed. Here, we examine decadal changes to seasonal processes that may contribute to this wide-reaching model bias using climate model simulations from the Community Earth System Model and below-ice observations from the Arctic Ice Dynamics Joint Experiment in 1975 and Ice Tethered Profilers in 2006–2012. In contrast to the observations, the models simulate salinity profiles that show relatively little variation between 1975 and 2012. We demonstrate that this bias can be mainly attributed to unrealistically deep vertical mixing in the model, creating a surface layer that is saltier than observed. The results provide insight for climate model improvement with broad implications for Arctic sea ice and ecosystem dynamics.

Plain Language Summary Climate models, which have been analyzed extensively to assess and predict current and future climate change and to inform policy, struggle to accurately simulate the rapid decline in Arctic sea ice. One possible source of this bias could be related to the vertical distribution of salt in the ocean, which controls the exchange of heat between the surface and deeper ocean. We compare simulations from two climate models to ocean observations collected below sea ice in the Canada Basin. In 1975, observations were collected by scientists living in ice camps, and in 2006–2012, they were obtained by automated instruments attached to sea ice. The observations indicate as much as six times greater surface freshening than the models between 1975 and 2006–2012. We show that the salt bias can be partly attributed to the models' tendency to mix fresh water from the surface deeper than in observations, resulting in a saltier ocean surface. The results may provide insight for climate model improvement that could have wide-reaching implications because the vertical distribution of salt in the ocean directly impacts the vertical transport of heat and nutrients.

1. Introduction

Rapid sea ice retreat has been extensively observed in the Canada Basin over the past several decades (F. McLaughlin et al., 2011). The increased sea ice melt and river runoff that has collected toward the center of the anticyclonic (convergent) Beaufort Gyre (Brown et al., 2020; E. C. Carmack et al., 2016; F. A. McLaughlin & Carmack, 2010; Proshutinsky et al., 2009; Wang et al., 2018; Yamamoto-Kawai et al., 2009) drive a 30-year 1.1–1.9 psu/yr trend toward a fresher surface layer (Peralta-Ferriz & Woodgate, 2015). The addition of this relatively light fresh water at the surface has stabilized the upper ocean, altering ice-ocean processes, including wind-driven mixing, the vertical transport of heat and nutrients, and sea ice basal melt (E. Carmack et al., 2015; Jackson et al., 2010, 2011; 2012; Steele et al., 2011; M. Timmermans & Marshall, 2020; M. L. Timmermans, 2015; Toole et al., 2010).

Historically, climate models simulate a slower sea ice retreat than observed (Niederdrenk & Notz, 2018; Rosenblum & Eisenman, 2016; SIMIP, 2020; Stroeve et al., 2007, 2012, 2017; Winton, 2011). One possible

10.1029/2021GL094739

source of the model bias could be related to simulated upper-ocean stratification, which tends to be less stratified in global ice-ocean models than in observations (Holloway et al., 2007; Ilicak et al., 2016). The ocean stratification bias could be related to unrealistic sea ice conditions, which could result in too little freshwater input from sea ice melt each season. Alternatively, the biases could be related to unrealistic ocean processes, such as vertical diffusion (Zhang & Steele, 2007) or brine rejection schemes (Nguyen et al., 2009). Up until now, this stratification bias has mainly been investigated with numerical experiments or by comparing simulations to annual climatologies with little to no attention paid to their seasonality (Barthélemy et al., 2015; Holloway et al., 2007; Ilicak et al., 2016; Jin et al., 2012; Nguyen et al., 2009; Sidorenko et al., 2018; Zhang & Steele, 2007).

Here, we explore this problem by examining both sea ice conditions and ocean processes in models and observations using simulations from the two most recent generations of the Community Earth System Model (CESM1 and CESM2), both of which are extensively used in polar studies and in the Intergovernmental Panel on Climate Change (IPCC) Fifth and Sixth Assessment Reports (AR5 and AR6), and using two sets of year-round ocean observations collected in the Canada Basin during 1975 and 2006–2012. Our main objective is to understand what governs the seasonal salinity evolution in the models and observations in the Canada Basin by examining seasonal surface processes related to sea ice conditions, freshwater input, and vertical mixing, all of which cumulatively contribute to decadal surface freshening. Distinguishing between atmospheric and oceanic processes that cause surface freshening in the models and observations is critical for determining if model freshening mechanisms are consistent with the natural world and helps to identify processes that might be missing or poorly simulated in the models.

2. Methods

We use year-round below-ice observations of ocean salinity collected in the Canada Basin, defined as the region enclosed by 72°N, 80°N, 130°W, and 155°W (Figure 1b), from the 1975 Arctic Ice Dynamics Joint Experiment (AIDJEX) program (Maykut & McPhee, 1995; Untersteiner et al., 2007) and during 2004-present from the Ice-Tethered Profiler (ITP) instrumentation system (Krishfield et al., 2008; Toole et al., 2011; 2016). There were four occupied AIDJEX ice camps between May 1975 and April 1976 and 30 ITPs, which were available for 2004–2012 at the time of the analysis. The data in this study are identical to those employed by Rosenblum et al. (2021), who showed that June-September surface changes between the ITP and AIDJEX datasets are consistent with 30-year mixed-layer trends reported by Peralta-Ferriz and Woodgate (2015) using data mainly associated with low sea ice concentration in the same region. They used only quality-controlled data (level 3) in the ITP archive, screened profiles to select those that include samples shallower than 10 m depth (as in Jackson et al., 2010), and that were collected during the period May 1 - December 31, which is common to both datasets. In total, 754 AIDJEX profiles during 1975 and 3391 ITP profiles during 2006–2012 from 12 ITPs (#1, 3–6, 8, 11, 13, 18, 33, 41, and 53) satisfied these criteria, with average shallowest measurements of ~6 m and ~7 m, respectively (Figure 1b). Profiles were linearly interpolated onto a common 1 m vertical grid, and the shallowest values were extrapolated to $z = 0$, which we take as the ice-ocean interface, as in the models.

To examine sea ice conditions associated with the ITP data set, we identify co-located daily sea ice concentrations, provided by the Passive Microwave satellite data, Version 1 (Cavalieri et al., 1996). Weekly, regional-mean sea ice concentrations associated with the AIDJEX data are provided by the Canadian Ice Service Digital Archive (CISDA) chart data for the western Arctic region (Tivy et al., 2011). We also examine estimates of the 1979–2018 effective sea ice thickness (sea ice volume per unit area) from the Pan Arctic Ice Ocean Modeling and Assimilation System (PIOMAS) (Schweiger et al., 2011). PIOMAS effective sea ice thickness was regridded to the 25-km Equal-Area Scalable Earth (EASE) grid, and data were collected from each grid cell residing in the Canada Basin. While several studies have shown that PIOMAS tends to underestimate sea ice thickness in regions of thicker ice and overestimate sea ice thickness in regions of thinner ice (Stroeve et al., 2014; Wang et al., 2018), the seasonality, spatial structure, distribution, and decadal trends of the sea ice thickness are realistically reproduced (Labe et al., 2018).

We use 30 simulations of 1970–2020 from CESM1 with historical and RCP8.5 forcing from the Large Ensemble project (Kay et al., 2015) and the first 50 CESM2 simulations from the Large Ensemble 2 project with

10.1029/2021GL094739

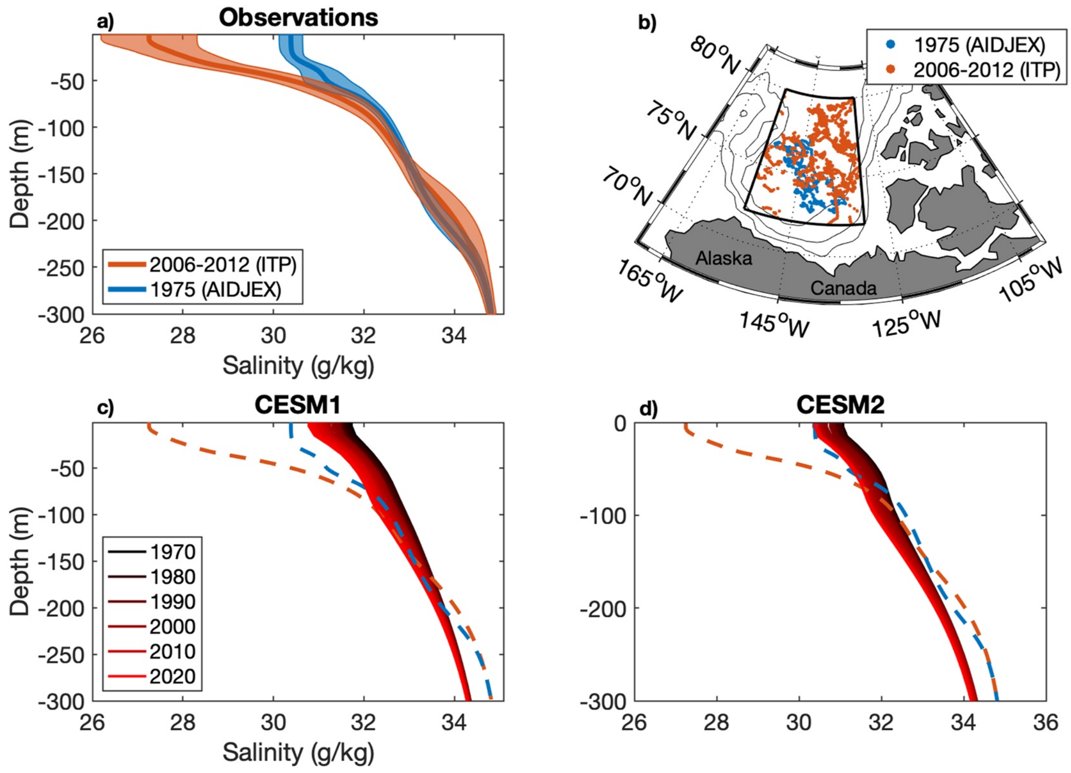

Figure 1. Observed salinity profiles from 1975 Arctic Ice Dynamics Joint Experiment (AIDJEX) data (blue) and 2006–2012 Ice-Tethered Profiler (ITP) data (red). Solid line indicates the May–December average and shading indicates one standard deviation. (b) Map showing the Canada Basin, the locations of 1975 AIDJEX data (blue) and 2006–2012 ITP data (red), and the region considered for this study (black lines). (c–d) Simulated May–December ensemble-mean basin average salinity profiles in 1970–2020 from (c) Community Earth System Model (CESM1) and (d) CESM2. AIDJEX (blue) and ITP (red) observations are repeated in panels (c, d).

historical and SSP 3–7.0 forcing (Rodgers et al., 2021). The CESM2 data was regridded onto a $1° \times 1°$ grid to facilitate the analysis. CESM1 and CESM2 are run with historical forcing until 2005 and 2015, respectively. Both models use the Parallel Ocean Program Version 2 (POP2) model with a displaced pole horizontal grid, a nominal 1° resolution, 60 vertical levels, and 10 m vertical grid spacing near the surface, although some of the physical parameterizations, including the K-profile parameterization (KPP) vertical ocean mixing scheme (Large et al., 1994), differ between the two models (Danabasoglu et al., 2020). We examine the ocean salinity, the effective sea ice thickness, and the sea ice concentration in each grid box within the Canada Basin of each simulation (Table S1 in Supporting Information S1).

3. Results

3.1. Upper-Ocean Salinity

The May–December average ocean salinity over the top 300 m in the models and the observations is shown in Figure 1. The observations indicate a significantly fresher upper ocean over the top 50 m in 2006–2012 than in 1975, with the largest differences occurring at the surface (Figure 1a), consistent with previous studies. By contrast, the 1970–2020 ensemble mean shows only a modest freshening from the surface down to 300 m in both models (Figures 1c and 1d). This results in a simulated upper-ocean stratification that is weaker than in recent observations, similar to most ice-ocean coupled models.

To eliminate the possibility that regional or internal variability could explain the bias, we examine the surface salinity from each observation and each grid point of each simulation during each month (Figure 2). In each dataset, we find a clear seasonal cycle where the surface becomes fresher in the summer and saltier in the fall, coinciding with seasonal sea ice evolution. In each month, we find that the models systematically

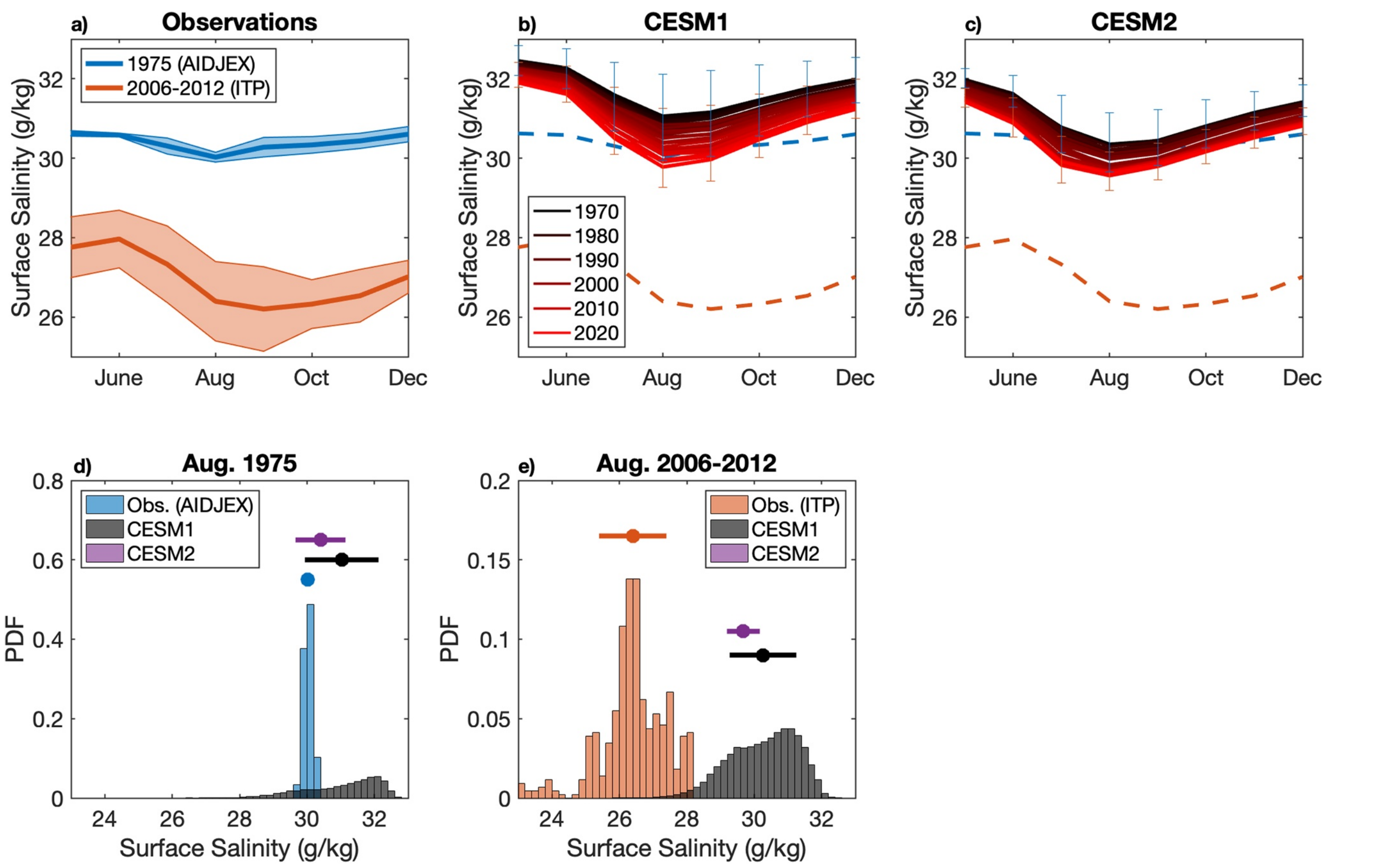

Figure 2. (a) Surface salinity from 1975 Arctic Ice Dynamics Joint Experiment (AIDJEX) data (blue) and 2006–2012 Ice Tethered Profiler (ITP) data (red). Solid line indicates the May–December average and shading indicates standard deviation. Blue and red error bars indicate one standard deviation over all grid points and simulations in 1975 and 2006–2012, respectively. (b–c) Simulated 1970–2020 ensemble-mean surface salinity from (b) Community Earth System Model (CESM1) and (c) CESM2. Distribution of August surface salinity in (d) 1975 and (e) 2006–2012 from each observation in 1975 (blue) and 2006–2012 (red), and from each grid point of each CESM1 (black) and CESM2 (purple) simulation of 1975 and 2006–2012 (distribution for CESM2 not shown). Solid dots and lines indicate mean and one standard deviation. AIDJEX (blue) and ITP (red) observations are repeated in panels (b, c).

simulate a 1970–2020 surface layer that is more consistent with observations in 1975 than in 2006–2012 (Figures 2b and 2c).

Focusing on August (the lowest monthly salinity in the models; Figures 2d and 2e; Table S2 in Supporting Information S1), we find that CESM1 indicates a 2006–2012 August surface layer that is only 0.7 ± 1.0 g/kg fresher than in 1975, similar to CESM2 (0.7 ± 0.9 g/kg). By contrast, the observations indicate an average 3.6 ± 1.0 g/kg change toward a fresher surface layer during the same time periods. As a consequence, we find that models are consistent with observations in 1975 but not in 2006–2012. From all simulations during August 2006–2012, only 1.4% of CESM1 grid cells and only 0.9% of CESM2 grid cells have a surface salinity that is as salty as any observation. We find similar results for other months (Figures S1 and S2 in Supporting Information S1) and after accounting for geographical differences between ITP and AIDJEX data (not shown).

Overall, Figures 1 and 2 show that the models do not simulate 1975 to 2006–2012 surface salinity change observed in the Canada Basin and that this bias cannot be explained by regional or internal variability present within the models. In the remainder of this section, we consider three factors related to seasonal surface processes to identify sources of the surface freshening model bias.

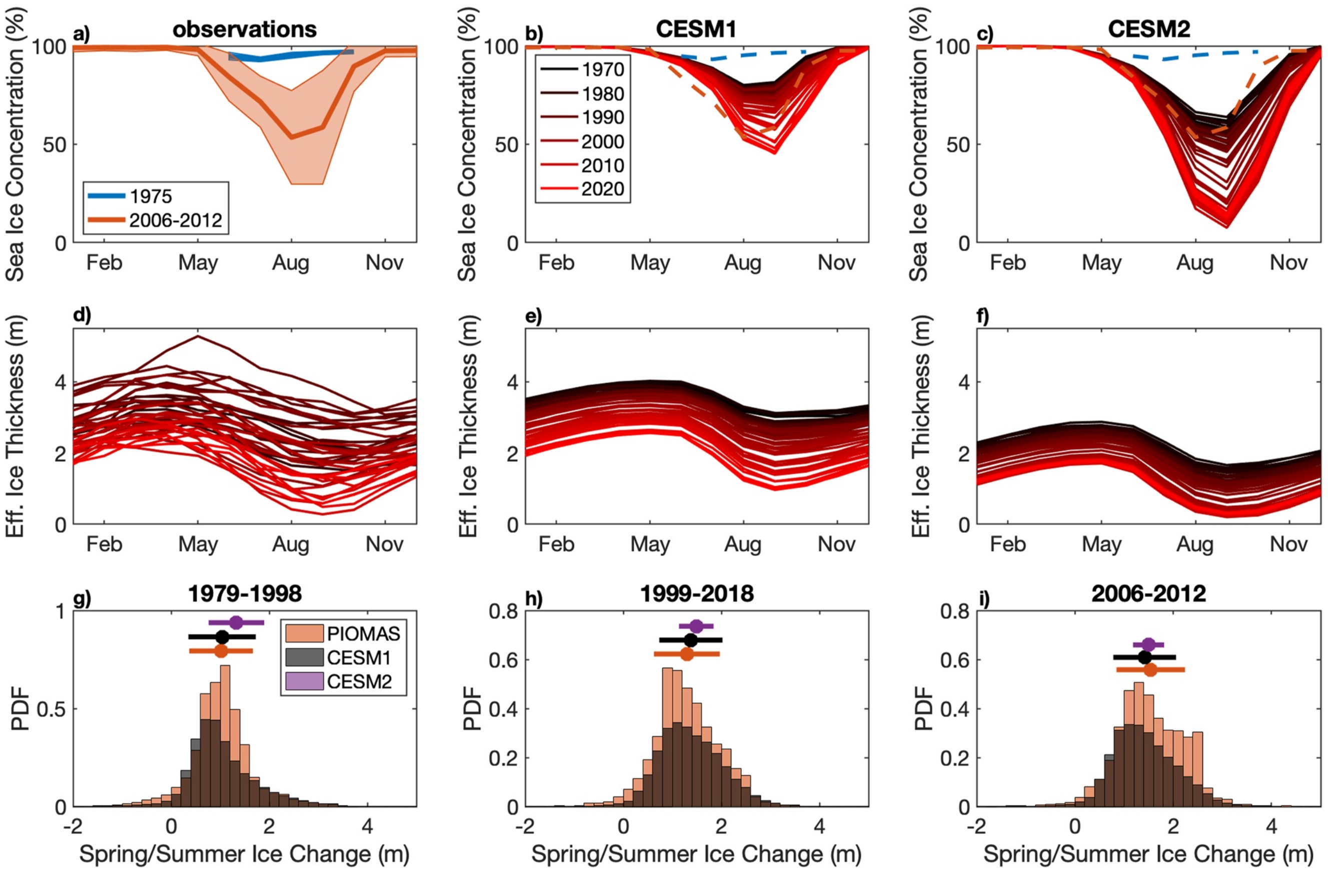

Figure 3. (a) Observed sea ice concentration co-located to 1975 Arctic Ice Dynamics Joint Experiment (AIDJEX) data (blue) and 2006–2012 Ice Tethered Profiler (ITP) data (red). Solid line indicates monthly mean, and shading indicates standard deviation. (b–c) Simulated 1970–2020 ensemble-mean sea ice concentration from (b) Community Earth System Model (CESM1) and (c) CESM2. (d–f) Effective sea ice thickness from (d) Pan Arctic Ice Ocean Modeling and Assimilation System (PIOMAS) and (e, f) CESM1 and CESM2 ensemble mean. (g–i) Distribution of the seasonal change of the effective sea ice thickness between May and September during (g) 1979–1998, (h) 1999–2018, and (i) 2006–2012 using all grid points from PIOMAS (red), and from each CESM1 (black) and CESM2 (purple) simulation (distribution for CESM2 not shown). Solid dots and lines indicate the mean and standard deviation. AIDJEX (blue) and ITP (red) observations are repeated in panels (b, c).

3.2. Sea Ice Conditions

Seasonal changes to the Arctic Ocean surface layer are primarily driven by the seasonal melting and freezing of sea ice (Lemke & Manley, 1984; McPhee & Smith, 1976; Morison & Smith, 1981; Peralta-Ferriz & Woodgate, 2015). In the models, the observations, and PIOMAS, we find a clear seasonal cycle and a considerable decline in both summer sea ice concentration (Figures 3a–3c) and effective sea ice thickness (Figures 3d–3f). To examine the decadal changes in seasonal sea ice volume evolution, which directly impacts the seasonal freshwater surface flux, we compute a seasonal change (September–May) in the effective ice thickness in each grid box in PIOMAS and in each simulation of CESM1 and CESM2 during 1979–2018 (Figures 3g–3i).

On average, PIOMAS, CESM1, and CESM2 indicate similar seasonal sea ice thickness changes during the melt season in 1979–1998 (0.9 ± 0.6 m, 0.8 ± 0.6 m, and 1.3 ± 0.6 m, respectively), in 1999–2018 (1.1 ± 0.6 m, 1.1 ± 0.6 m, and 1.5 ± 0.4 m, respectively), and in 2006–2012 (1.5±0.7 m, 1.4 ± 0.6 m, and 1.5 ± 0.3 m, respectively). These results suggest that CESM1 and CESM2 are able to realistically simulate the seasonal sea ice volume evolution in the Canada Basin, consistent with previous studies (see references in Methods). This suggests that, while there are differences in sea ice concentration between the models and observations (Figures 3a–3c; Table S2 in Supporting Information S1), seasonal sea ice volume biases are unlikely to explain the surface freshening model bias (Figures 1 and 2).

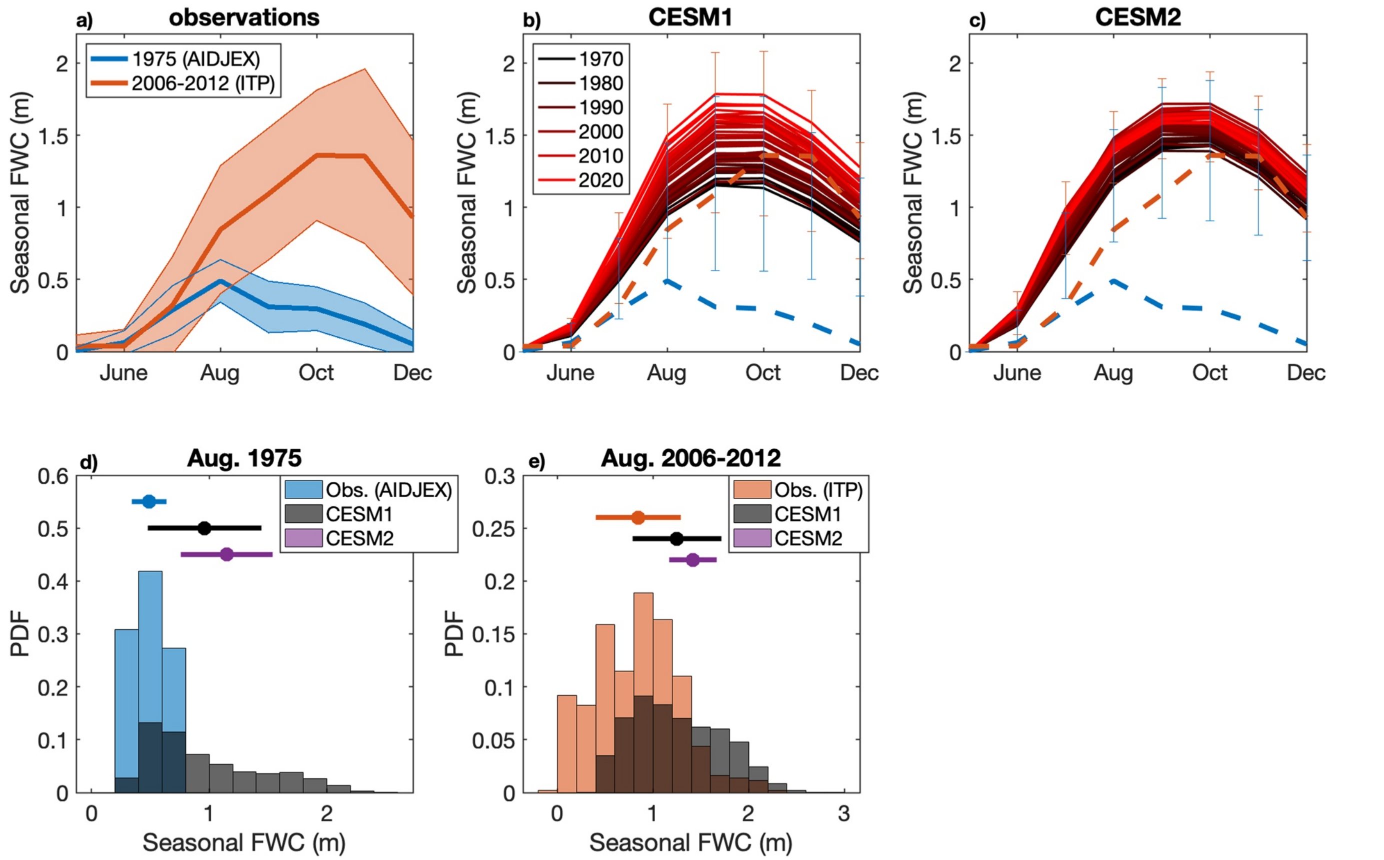

Figure 4. (a) Observed sFWC from 1975 Arctic Ice Dynamics Joint Experiment (AIDJEX) data (blue) and 2006–2012 Ice-Tethered Profiler (ITP) data (red). Solid line indicates monthly-mean and shading indicates one standard deviation. (b–c) Simulated 1970–2020 ensemble-mean sFWC from (b) Community Earth System Model (CESM1) and (c) CESM2. Blue and red error bars indicate one standard deviation over all grid points and simulations in 1975 and 2006–2012, respectively. (d–e) Distribution of August sFWC in (d) 1975 and (e) 2006–2012 from each observation in 1975 (blue) and 2006–2012 (red), and from each grid point of each CESM1 (black) and CESM2 (purple) simulation of 1975 and 2006–2012 (distribution for CESM2 not shown). Solid dots and lines indicate mean and one standard deviation. AIDJEX (blue) and ITP (red) observations are repeated in panels (b, c).

3.3. Seasonal Freshwater Storage

We next estimate the amount of fresh water stored seasonally in the upper ocean by examining the seasonal evolution of the observed and simulated salinity profiles, which reflects any process that drives changes to the upper-ocean salinity, including sea ice melt, river runoff, precipitation, or advection. Specifically, we use the upper-ocean seasonal freshwater content relative to May-average conditions (sFWC), given by:

$$\mathrm{sFWC}(t) = \int_{Z_{fw}(t)}^{0} \frac{S_{\mathrm{May}} - S(t,z)}{S_{\mathrm{May}}} dz, \tag{1}$$

where S is salinity, and Z_{fw} indicates the vertical extent of mixing defined by $S(Z_{fw}) = S_{\mathrm{May}}$, where z and Z_{fw} are both negative. S_{May} is the May-average surface salinity, which is computed separately for each grid box of each year in each model simulation and is computed separately for each ITP or AIDJEX ice camp of each year in the observations. We compute sFWC from May–December at each grid point in each simulation of 1970–2020 from each model and for each observation in 1975 and 2006–2012 (Figure 4). The value sFWC, therefore, represents the amount of fresh water necessary to explain the transition from a well-mixed May salinity profile (S_{May}) to any subsequent profile ($S(t,z)$) for $z \geq Z_{fw}$ at a given location in the models or observations. Figure S3 in Supporting Information S1 shows examples of this calculation from single profiles.

The expression for sFWC differs from the more often used expression for freshwater content in which the reference salinity is set to 34.8 g/kg. Instead, we use a reference salinity that is set to the May-average surface salinity. This difference implies that sFWC reflects the seasonal near-surface freshwater content over a well-defined volume (see SI for full derivation of sFWC), which avoids errors that can arise when using an arbitrary reference salinity (Schauer & Losch, 2019). Furthermore, we use the same criterion for S_{May} in both the models and observations, allowing for a fair comparison.

In both models and observations, we find that the average sFWC increases through the summer and into the fall, coinciding with the summer melt season, river runoff, and the intensification of the convergent Beaufort Gyre circulation. In late fall and early winter, both the models and observations indicate an average decrease of sFWC, coinciding with brine rejection from freeze-up. As given in Section 3.1, we consider the distribution of the sFWC from every observation and from every grid point of every simulation in August 1975 and 2006–2012 (Figures 4d and 4e). We find that, on average, the August sFWC is 0.4–0.5 m larger in the models than in the observations during both time periods (Table S2 in Supporting Information S1). We find similar results for other months, with the bias decreasing in fall 2006–2012 and increasing in fall 1975 (Figures 4a–4c and S4 and S5 in Supporting Information S1). Together, this causes a smaller change in sFWC between 2006–2012 and 1975 in the models than in the observations.

We note that the simulated internal variability appears to be smaller in CESM2 than in CESM1 (compare standard deviations in Figures 2–4). This could be related to differences in climate sensitivity, which causes a reduced sea ice volume in CESM2 than in CESM1 (DeRepentigny et al., 2020; Figures 3b, 3c, 3e and 3f) and thus a reduced variability in freshwater input and surface salinity.

Overall, we find that the models appear to simulate somewhat more fresh water stored near the surface on seasonal timescales than observed. This suggests that, while there are differences in sFWC between the models and observations, insufficient seasonal freshwater input at the surface is not the likely source of the bias toward too little surface freshening in the model (Figures 1 and 2).

3.4. Vertical Freshwater Distribution

Qualitatively, the average 2006–2012 seasonal salinity evolution indicates seasonal freshwater input is stored deeper in the models than in observations (Figure 5i). To quantify this difference, we examine the vertical distribution of seasonal freshwater storage in the models and observations during every month by rewriting the expression for sFWC as:

$$\mathrm{sFWC} = \underbrace{\int_{Z_{10\%}}^{0} \frac{S_{\mathrm{May}} - S(z)}{S_{\mathrm{May}}}\,dz}_{=10\%\text{ of sFWC}} + \underbrace{\int_{Z_{20\%}}^{Z_{10\%}} \frac{S_{\mathrm{May}} - S(z)}{S_{\mathrm{May}}}\,dz}_{=10\%\text{ of sFWC}} + \& + \underbrace{\int_{Z_{fw}}^{Z_{90\%}} \frac{S_{\mathrm{May}} - S(z)}{S_{\mathrm{May}}}\,dz}_{=10\%\text{ of sFWC}}, \tag{2}$$

where $Z_{10\%}, Z_{20\%}, \ldots, Z_{fw}$ is the lower bound of the depth range that encompasses 10%, 20%,...,100% of the sFWC. These depths are computed at each grid point of each simulation and each observation during May–December of 1975 and 2006–2012 (Figure 5). We only include data points with positive values of sFWC, implying that some observed June profiles are not included in this portion of the analysis. As given in Section 3.3, we also consider the August distribution of $Z_{90\%}$ from every observation and from every grid point of every simulation in 1975 and 2006–2012 (Figures 5g and 5h; Table S2 in Supporting Information S1). $Z_{90\%}$ is closely related to the mixed-layer depth in both the models and observations from July onward, when sFWC is large enough to form a well-defined summer mixed layer (Figure S6 in Supporting Information S1). We use $Z_{90\%}$ instead of the more commonly used mixed-layer depth because its value can vary based on its definition (Peralta-Ferriz & Woodgate, 2015) and because the precise definition of $Z_{90\%}$ is both physically relevant and can be calculated in the same way for both models and observations.

The vertical distribution of sFWC reveals two main discrepancies between the models and observations (Figure 5). First, we find that the fresh water is spread over a deeper range in the simulations (Aug. $Z_{90\%} = 24 \pm 2.7$ m, 26 ± 3.1 m in CESM1, CESM2) compared to the observations (Aug. $Z_{90\%} = 14 \pm 3.7$ m) in 2006–2012. Second, we find that the vertical distribution of sFWC remains relatively unchanged between 1975 and 2006–2012 in the simulations (less than 1 m change in August $Z_{90\%}$), while the observations indicate that the fresh water is concentrated significantly closer to the surface in 2006–2012 than in 1975 (~8 m change).

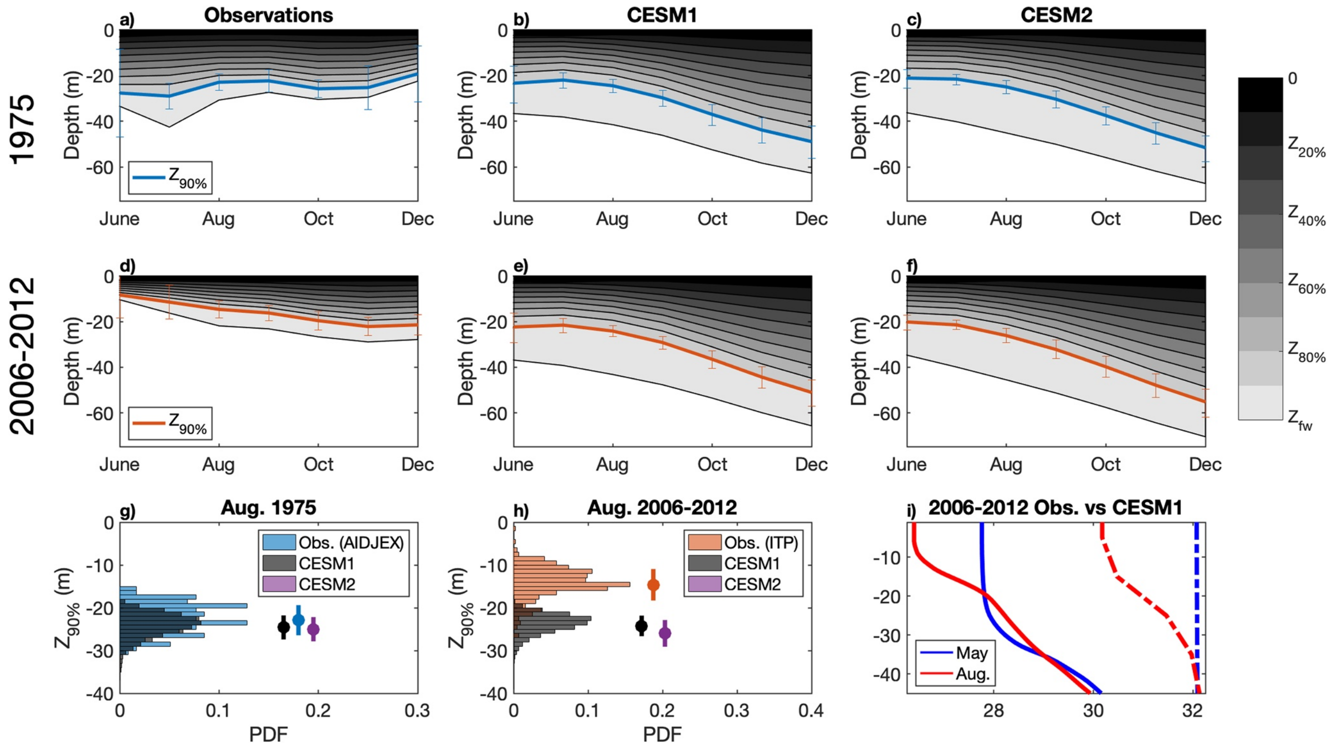

Figure 5. (a–f) Black solid lines separating each gray shading indicate the monthly-average depths of $Z_{10\%}, Z_{20\%}, \ldots, Z_{fw}$ (Equation 2) from (a, d) observations, (b, e) Community Earth System Model (CESM1) ensemble-mean, and (c, f) CESM2 ensemble mean in (a–c) 1975 and (d–f) 2006–2012. Dashed lines indicate $Z_{90\%}$ in 1975 (a–c, blue) and 2006–2012 (d–f, red). Blue and red error bars indicate one standard deviation over all grid points and simulations in 1975 and 2006–2012, respectively. (g–h) Distribution of August $Z_{90\%}$ in (g) 1975 and (h) 2006–2012 from each observation 1975 (blue) and 2006–2012 (red), and from each grid point of each CESM1 (black) and CESM2 (purple) simulation of 1975 and 2006–2012 (distribution for CESM2 not shown). Solid dots and lines indicate mean and one standard deviation. (i) Simulated (dashed) and observed (solid) salinity profiles averaged over May (blue) and August (red) of 2006–2012.

Interestingly, we also find that the models do simulate a 1975 vertical distribution of sFWC consistent with the observations during the summer (Aug. $Z_{90\%} = 23 \pm 3.5$ m, 25 ± 2.8 m, and 25 ± 2.8 m in the observations, CESM1, and CESM2, respectively), similar to the 1975 surface salinity (Figures 1 and 2). However, an unrealistically large amount of fresh water (Figure 4) is stored unrealistically deep in later months (Figure 5), suggesting that this is a result of compensating errors.

Overall, we find that the 2006–2012 seasonal freshwater storage has an unrealistic vertical distribution in the models and that the discrepancy between the models and observations cannot be explained by regional or internal variability present within the models (Figures 5g and 5h). Together this suggests that simulated vertical mixing of fresh water is inconsistent with observations in recent years and that this is a source of the surface freshening model bias (Figures 1 and 2).

4. Conclusions

State-of-the-art coupled ice-ocean models struggle to accurately simulate upper-ocean stratification in the Canada Basin, and instead tend to simulate a surface layer that is saltier and less stratified than observed (Holloway et al., 2007; Ilicak et al., 2016). The bias could be related to sea ice, atmospheric, or ocean processes and, until now, had only been examined using numerical experiments and annual climatologies (Barthélemy et al., 2015; Holloway et al., 2007; Ilicak et al., 2016; Jin et al., 2012; Nguyen et al., 2009; Sidorenko et al., 2018; Zhang & Steele, 2007). Here, we examine this question by focusing on decadal changes to seasonal surface processes using observations from below-ice ocean measurements collected during May–December 1975 (AIDJEX) and 2006–2012 (ITPs) and in the two most recent generations of the Community Earth Systems Models (CESM1 and CESM2).

We find that CESM1 and CESM2 have an upper-ocean stratification bias in 2006–2012, similar to most global ice-ocean models, but with an upper-ocean stratification that is fairly consistent with observations in 1975 (Figures 1 and 2). That is, the models fail to capture the fresh surface layer that appears in recent years. We show that this surface freshening model bias is likely related to the unrealistically deep mixing of fresh water in the models (Figure 5), rather than biases related to sea ice conditions (Figure 3) or insufficient seasonal freshwater input (Figure 4). This suggests that one source of the 2006–2012 ocean stratification bias is closely related to missing or unrealistic mixed-layer dynamics in recent years, rather than unrealistic sea ice conditions or seasonal freshwater input from ice melt, river-runoff, precipitation, advection, or other sources. These results are independent of differences in climate sensitivity and sea ice conditions between CESM1 and CESM2 (DeRepentigny et al., 2020; Figure 3), and also do not depend on differences in sea ice concentration between the models and observations (Figures S7–S8 in Supporting Information S1).

This result raises important questions as to what mechanisms must be included in climate models to simulate the decadal trend toward a shallower summer mixed layer in recent years. Previous studies have indicated that simulated vertical mixing is sensitive to several interconnected processes, including Ekman dynamics (Zhang & Steele, 2007), vertical mixing schemes (Liang & Losch, 2018), and ice-ocean momentum transfer (Dewey et al., 2018; Meneghello, Marshall, Campin, et al., 2018; Meneghello, Marshall, Timmermans, & Scott, 2018), and are directly linked to the representation of Atlantic Water circulation (Zhang & Steele, 2007). Identifying the role of each mechanism and improving their modeled representation will be particularly important in regions such as the Canada Basin, where the summer mixed-layer depth can be smaller than the vertical resolution in the models (~10 m). This is an interesting direction for future study.

Because the upper-ocean stratification directly impacts the vertical exchange of heat, energy, and nutrients, these results may have important implications for Arctic ecosystem dynamics and for sea ice cover. For example, if the unrealistically deep transport of fresh water carries heat downward and traps nutrients deeper, then there could be less heat available for summer sea ice melt, a weaker seasonal ice-albedo feedback, and reduced primary productivity. These results, therefore, highlight the need for improved parameterizations of upper-ocean dynamics under a rapidly changing sea ice cover.

Data Availability Statement

The AIDJEX data used in this study can be found at http://lwbin-datahub.ad.umanitoba.ca/dataset/aidjex. The Ice-Tethered Profiler data were collected and made available by the Ice-Tethered Profiler Program based at the Woods Hole Oceanographic Institution and can be found at https://www2.whoi.edu/site/itp/data/. All sea ice concentration data created or used during this study are openly available from the NASA National Snow and Ice Data Center Distributed Active Archive Center at https://doi.org/10.5067/8GQ8LZQVL0VL. More information on each data source is listed in the methods and references. The data on which this article is based are fully described in Cavalieri et al. (1996); Danabasoglu et al. (2020); Krishfield et al. (2008); Maykut and Untersteiner (1971); Kay et al. (2015); Schweiger et al. (2011); Tivy et al. (2011); Toole et al. (2011, 2016); Untersteiner et al. (2007).

Acknowledgments

ER was supported by the National Sciences and Engineering Research Council of Canada (NSERC) PDF award. ER and JS were supported by the NSERC Canada-150 Chair (Award G00321321). STG was supported by the US NSF (Awards PLR-1425989 and OPP-1936222) and by the US Department of Energy (DOE) (Award DE-SC0020073). This work is a contribution to the NSERC—Discovery Grant and the NSF Office of Polar Program grant # 1504023 awarded to LBT. RG was supported by the NSERC Canada Discovery Grant program. RF acknowledges funding from NSERC Canada through a CGS-D award, the US DOE (Grant DE-SC001940), and the NOAA Climate and Global Change Postdoctoral Fellowship Program, administered by UCAR's Cooperative Program for the Advancement of Earth System Sciences (Award #NA18NWS4620043B). The authors thank Benjamin Rabe and Chris Horvat for helpful comments and suggestions.

References

Barthélemy, A., Fichefet, T., Goosse, H., & Madec, G. (2015). Modeling the interplay between sea ice formation and the oceanic mixed layer: Limitations of simple brine rejection parameterizations. *Ocean Modelling*, *86*, 141–152. https://doi.org/10.1016/j.ocemod.2014.12.009

Brown, K. A., Holding, J. M., & Carmack, E. C. (2020). Understanding regional and seasonal variability is key to gaining a pan-Arctic perspective on Arctic Ocean freshening. *Frontiers of Marine Sciences*, *7*, 606. https://doi.org/10.3389/fmars.2020.00606

Carmack, E., Polyakov, I., Padman, L., Hunke, E., Hutchings, J., et al. (2015). Towards quantifying the increasing role of oceanic heat in sea ice loss in the New Arctic. *Bulletin of the American Meteorological Society*, *96*(12). https://doi.org/10.1175/BAMS-D-13-00177.1

Carmack, E. C., Yamamoto-Kawai, M., Haine, T. W. N., Bacon, S., Bluhm, B. A., Lique, C., et al. (2016). Freshwater and its role in the Arctic Marine System: Sources, disposition, storage, export, and physical and biogeochemical consequences in the Arctic and global oceans. *Journal of Geophysical Research: Biogeosciences*, *121*, 675–717. https://doi.org/10.1002/2015JG003140

Cavalieri, D., Parkinson, C. L., Gloersen, P., & Zwally, H. J. (1996). *sea ice concentrations from SMMR and DMSP SSMI/I-SSMIS Passive Microwave data. Version1. Natl. Snow and ice data cent*. Retrieved from https://nsidc.org/data/nsidc-0051

Danabasoglu, G., Lamarque, J. F., Bacmeister, J., Bailey, D. A., DuVivier, A. K., Edwards, J., et al. (2020). The Community Earth System Model Version 2 (CESM2). *Journal of Advances in Modeling Earth Systems*, *12*(2), 1–35. https://doi.org/10.1029/2019MS001916

DeRepentigny, P., Jahn, A., Holland, M. M., & Smith, A. (2020). Arctic sea ice in two configurations of the cesm2 during the 20th and 21st centuries. *Journal of Geophysical Research: Oceans*, *125*(9), e2020JC016133. https://doi.org/10.1029/2020jc016133

Dewey, S., Morison, J., Kwok, R., Dickinson, S., Morison, D., & Andersen, R. (2018). Arctic ice-ocean coupling and gyre equilibration observed with remote sensing. *Geophysical Research Letters*, *45*, 1499–1508. https://doi.org/10.1002/2017GL076229

Holloway, G., Dupont, F., Golubeva, E., Häkkinen, S., Hunke, E., Jin, M., et al. (2007). Water properties and circulation in Arctic Ocean models. *Journal of Geophysical Research: Oceans*, *112*(4), 1–18. https://doi.org/10.1029/2006JC003642

Ilicak, M., Drange, H., Wang, Q., Gerdes, R., Aksenov, Y., Bailey, D., & Yeager, S. G. (2016). An assessment of the Arctic Ocean in a suite of interannual CORE-II simulations. Part III: Hydrography and fluxes. *Ocean Modelling*, *100*, 141–161.

Jackson, J. M., Allen, S. E., McLaughlin, F. A., Woodgate, R. A., & Carmack, E. C. (2011). Changes to the near-surface waters in the Canada Basin, Arctic Ocean from 1993-2009: A basin in transition. *Journal of Geophysical Research*, *116*, 1–21. https://doi.org/10.1029/2011JC007069

Jackson, J. M., Carmack, E. C., McLaughlin, F. A., Allen, S. E., & Ingram, R. G. (2010). Identification, characterization, and change of the near-surface temperature maximum in the Canada Basin, 1993-2008. *Journal of Geophysical Research*, *115*, 1–16. https://doi.org/10.1029/2009JC005265

Jackson, J. M., Williams, W. J., & Carmack, E. C. (2012). Winter sea-ice melt in the Canada Basin, Arctic ocean. *Geophysical Research Letters*, *39*, L03603. https://doi.org/10.1029/2011GL050219

Jin, M., Hutchings, J., Kawaguchi, Y., & Kikuchi, T. (2012). Ocean mixing with lead-dependent subgrid scale brine rejection parameterization in a climate model. *Journal of Ocean University of China*, *11*(4), 473–480. https://doi.org/10.1007/s11802-012-2094-4

Kay, J. E., Deser, C., Phillips, A., Mai, A., Hannay, C., Strand, G., et al. (2015). The community earth system model (CESM) large ensemble project : A community resource for studying climate change in the presence of internal climate variability. *Bulletin of the American Meteorological Society*, *96*, 1333–1349. https://doi.org/10.1175/BAMS-D-13-00255.1

Krishfield, R., Toole, J., Proshutinsky, A., & Timmermans, M. L. (2008). Automated ice-tethered profilers for seawater observations under pack ice in all seasons. *Journal of Atmospheric and Oceanic Technology*, *25*(11), 2091–2105. https://doi.org/10.1175/2008JTECHO587.1

Labe, Z., Magnusdottir, G., & Stern, H. (2018). Variability of Arctic sea ice thickness using PIOMAS and the CESM large ensemble. *Journal of Climate*, *31*(8), 3233–3247. https://doi.org/10.1175/JCLI-D-17-0436.1

Large, W. G., McWilliams, J. C., & Doney, S. C. (1994). Oceanic vertical mixing: A review and a model with a nonlocal boundary layer parameterization. *Reviews of Geophysics*, *34*(4), 363–403. https://doi.org/10.1029/94RG01872

Lemke, P., & Manley, T. O. (1984). The seasonal variation of the mixed layer and the pycnocline under polar sea ice. *Journal of Geophysical Research*, *89*, 6494. https://doi.org/10.1029/JC089iC04p06494

Liang, X., & Losch, M. (2018). On the effects of increased vertical mixing on the arctic ocean and sea ice. *Journal of Geophysical Research: Oceans*, *123*(12), 9266–9282. https://doi.org/10.1029/2018jc014303

Maykut, G. A., & McPhee, M. G. (1995). Solar heating of the Arctic mixed layer. *Journal of Geophysical Research*, *100*, 24691. https://doi.org/10.1029/95JC02554

Maykut, G. A., & Untersteiner, N. (1971). Some results from a time-dependent thermodynamic model of sea ice. *Journal of Geophysical Research*, *76*(6), 1550–1575. https://doi.org/10.1029/jc076i006p01550

McLaughlin, F., Carmack, E., Proshutinsky, A., Krishfield, R., Guay, C., Yamamoto-Kawai, M., et al. (2011). The rapid response of the Canada Basin to climate forcing. *Oceanography*, *24*, 136–159. https://doi.org/10.5670/oceanog.2011.66

McLaughlin, F. A., & Carmack, E. C. (2010). Deepening of the nutricline and chlorophyll maximum in the Canada Basin interior, 2003-2009. *Geophysical Research Letters*, *37*(24), L24602. https://doi.org/10.1029/2010GL045459

McPhee, M. G., & Smith, J. D. (1976). Measurements of the turbulent boundary layer under pack ice. *Journal of Physical Oceanography*, *6*, 696–711. https://doi.org/10.1175/1520-0485(1976)006⟨0696:MOTTBL⟩2.0.CO;2

Meneghello, G., Marshall, J., Campin, J. M., Doddridge, E., & Timmermans, M. L. (2018). The ice-ocean governor: Ice-ocean stress feedback limits Beaufort Gyre Spin-Up. *Geophysical Research Letters*, *45*(11), 11293–11299. https://doi.org/10.1029/2018GL080171

Meneghello, G., Marshall, J., Timmermans, M. L., & Scott, J. (2018). Observations of seasonal upwelling and downwelling in the Beaufort Sea mediated by sea ice. *Journal of Physical Oceanography*, *48*(4), 795–805. https://doi.org/10.1175/JPO-D-17-0188.1

Morison, J., & Smith, J. D. (1981). Seasonal variations in the upper Arctic Ocean as observed at T-3. *Geophysical Research Letters*, *8*, 753–756. https://doi.org/10.1029/GL008i007p00753

Nguyen, A. T., Menemenlis, D., & Kwok, R. (2009). Improved modeling of the arctic halocline with a subgrid-scale brine rejection parameterization. *Journal of Geophysical Research*, *114*(11), 1–12. https://doi.org/10.1029/2008JC005121

Niederdrenk, A. L., & Notz, D. (2018). Arctic sea ice in a 1.5C warmer world. *Geophysical Research Letters*, *45*(4), 1963–1971. https://doi.org/10.1002/2017GL076159

Peralta-Ferriz, C., & Woodgate, R. A. (2015). Seasonal and interannual variability of pan-Arctic surface mixed layer properties from 1979 to 2012 from hydrographic data, and the dominance of stratification for multiyear mixed layer depth shoaling. *Progress in Oceanography*, *134*, 19–53. https://doi.org/10.1016/j.pocean.2014.12.005

Proshutinsky, A., Krishfield, R., Timmermans, M.-L., Toole, J., Carmack, E., McLaughlin, F., et al. (2009). Beaufort Gyre freshwater reservoir: State and variability from observations. *Journal of Geophysical Research*, *114*, C00A10. https://doi.org/10.1029/2008JC005104

Rodgers, K. B., Lee, S.-S., Rosenbloom, N., Timmermann, A., Danabasoglu, G., & Deser, C. (2021). Ubiquity of human-induced changes in climate variability. *Earth System Dynamics Discussions*, 1–22.

Rosenblum, E., & Eisenman, I. (2016). Faster Arctic sea ice retreat in CMIP5 than in CMIP3 due to volcanoes. *Journal of Climate*, *29*(24), 9179–9188. https://doi.org/10.1175/JCLI-D-16-0391.1

Rosenblum, E., & Eisenman, I. (2017). Sea ice trends in climate models only accurate in runs with biased global warming. *Journal of Climate*, *30*(16), 6265–6278. https://doi.org/10.1175/JCLI-D-16-0455.1

Rosenblum, E., Stroeve, J. S., Gille, S., Tremblay, L., Carmack, E. C., Barber, D. G., et al. (2021). *Freshwater input and vertical distribution in the Canada Basin's seasonal halocline: 1975 versus 2006-2012*. https://doi.org/10.1002/essoar.10507192.1

Schauer, U., & Losch, M. (2019). Freshwater in the ocean is not a useful parameter in climate research. *Journal of Physical Oceanography*, *49*(9), 2309–2321. https://doi.org/10.1175/JPO-D-19-0102.1

Schweiger, A., Lindsay, R., Zhang, J., Steele, M., & Stern, H. (2011). Uncertainty in modeled Arctic sea ice volume. *Journal of Geophysical Research*, *116*(C8), C00D06. https://doi.org/10.1029/2011jc007084

Sidorenko, D., Koldunov, N. V., Wang, Q., Danilov, S., Goessling, H. F., Gurses, O., et al. (2018). Influence of a salt plume parameterization in a coupled climate model. *Journal of Advances in Modeling Earth Systems*, *10*(9), 2357–2373. https://doi.org/10.1029/2018MS001291

SIMIP. (2020). Arctic sea ice in CMIP6. *Geophysical Research Letters*, *47*(10), e2019GL086749. https://doi.org/10.1029/2019gl086749

Steele, M., Ermold, W., & Zhang, J. (2011). Modeling the formation and fate of the near-surface temperature maximum in the Canadian Basin of the Arctic Ocean. *Journal of Geophysical Research*, *116*, C11015. https://doi.org/10.1029/2010JC006803

Stroeve, J., Barrett, A., Serreze, M., & Schweiger, A. (2014). Using records from submarine, aircraft and satellites to evaluate climate model simulations of Arctic sea ice thickness. *The Cryosphere*, *8*(5), 1839–1854. https://doi.org/10.5194/tc-8-1839-2014

Stroeve, J., Holland, M. M., Meier, W., Scambos, T., & Serreze, M. (2007). Arctic sea ice decline: Faster than forecast. *Geophysical Research Letters*, *34*, L09501. https://doi.org/10.1029/2007GL029703

Stroeve, J., Kattsov, V., Barrett, A., Serreze, M., Pavlova, T., Holland, M., & Meier, W. N. (2012). Trends in Arctic sea ice extent from CMIP5, CMIP3 and observations. *Geophysical Research Letters*, *39*, L16502. https://doi.org/10.1029/2012GL052676

Timmermans, M., & Marshall, J. (2020). Understanding Arctic ocean circulation: A review of ocean dynamics in a changing climate. *Journal of Geophysical Research: Oceans*, *125*, 1–35. https://doi.org/10.1029/2018jc014378

Timmermans, M. L. (2015). The impact of stored solar heat on Arctic sea ice growth. *Geophysical Research Letters*, *42*, 6399–6406. https://doi.org/10.1002/2015GL064541

Tivy, A., Howell, S. E., Alt, B., McCourt, S., Chagnon, R., Crocker, G., et al. (2011). Trends and variability in summer sea ice cover in the Canadian Arctic based on the Canadian Ice Service Digital Archive, 1960-2008 and 1968-2008. *Journal of Geophysical Research: Oceans*, *116*, C03007. https://doi.org/10.1029/2009JC005855

Toole, J. M., Krishfield, R. A., & Woods Hole Oceanographic Institution Ice-Tethered Profiler Program. (2016). *Ice-Tethered Profiler observations: Vertical profiles of salinity from an Ice-Tethered Profiler buoy system*. NOAA National Centers for Environmental Information. Dataset. https://doi.org/10.7289/v5mw2f7x

Toole, J. M., Krishfield, R. A., Timmermans, M. L., & Proshutinsky, A. (2011). The ice-tethered profiler: Argo of the Arctic. *Oceanography*, *24*(3), 126–135. https://doi.org/10.5670/oceanog.2011.64

Toole, J. M., Timmermans, M. L., Perovich, D. K., Krishfield, R. A., Proshutinsky, A., & Richter-Menge, J. A. (2010). Influences of the ocean surface mixed layer and thermohaline stratification on Arctic Sea ice in the central Canada Basin. *Journal of Geophysical Research: Oceans*, *115*, 1–14. https://doi.org/10.1029/2009JC005660

Untersteiner, N., Thorndike, A. S., Rothrock, D. A., & Hunkins, K. L. (2007). AIDJEX revisited: A look back at the U.S.-Canadian Arctic Ice Dynamics Joint Experiment 1970-78. *Arctic*, *60*, 327–336. https://doi.org/10.14430/arctic233

Wang, Q., Wekerle, C., Danilov, S., Koldunov, N., Sidorenko, D., Sein, D., et al. (2018). Arctic sea ice decline significantly contributed to the unprecedented liquid freshwater accumulation in the Beaufort Gyre of the Arctic Ocean. *Geophysical Research Letters*, *45*(10), 4956–4964. https://doi.org/10.1029/2018GL077901

Winton, M. (2011). Do climate models underestimate the sensitivity of northern hemisphere sea ice cover? *Journal of Climate*, *24*, 3924–3934. https://doi.org/10.1175/2011JCLI4146.1

Yamamoto-Kawai, M., McLaughlin, F. A., Carmack, E. C., Nishino, S., Shimada, K., & Kurita, N. (2009). Surface freshening of the Canada Basin, 2003-2007: River runoff versus sea ice meltwater. *Journal of Geophysical Research*, *114*, C00A05. https://doi.org/10.1029/2008JC005000

Zhang, J., & Steele, M. (2007). Effect of vertical mixing on the Atlantic Water layer circulation in the Arctic Ocean. *Journal of Geophysical Research*, *112*(4), 1–9. https://doi.org/10.1029/2006JC003732